

# NANO-ENHANCED IMPACT PROPERTIES OF CARBON FIBRE REINFORCED COMPOSITES

V. Kostopoulos <sup>1</sup>, A. Baltopoulos <sup>1</sup>, P. Karapappas <sup>1</sup>, A. Vavouliotis <sup>1</sup> and A. Paipetis <sup>2</sup>

<sup>1</sup> *Applied Mechanics Laboratory, Department of Mechanical Engineering and Aeronautics, University of Patras, 26500, Patras, Greece*

<sup>2</sup> *Department of Materials Science & Engineering, University of Ioannina, P.O. Box 1186, GR-45110 Ioannina, Greece*

**KEYWORDS:** impact, carbon nanotubes, damage tolerance, CFRP.

## ABSTRACT

The exceptional properties of CNTs were investigated under impact loading. Carbon reinforced quasi-isotropic laminates doped with 0.5% MWCNTs per weight into the polymer matrix were subjected to low energy impacts and directly compared with an undoped panel. Even though the CNTs greatly enhance the fracture properties of CFRPs, their contribution to the improvement of the impact properties was only worth mentioning for the higher energy levels. Moreover, the two panels were subjected to compression after loading testing where the CNT doped panel demonstrated superior properties of about 13-17% for the effective compression modulus.

## 1. INTRODUCTION

The damage tolerance concept in aerospace structures relates to their ability to perform to required standards within damage limits, which at the same time define its remaining life time. This is the main design criterion for composite structures which are exposed to a number of events during in-service loading, which can cause damage initiation and structural degradation. Impact (low or high velocity) during service is a common phenomenon for aerospace composite structures. On impact, the incident energy is absorbed by a variety of mechanisms [1-3], but to produce an impact resistant component, the amount of energy absorbed through damage should be minimised. Generally, the first fracture event during an impact is the formation of matrix cracks within the plies, caused by through-thickness shear stresses generated by the out-of-plane impact forces. The dominant failure mode during low velocity impact that of delamination, can be split into two aspects; initiation and propagation. Delaminations are usually initiated by opening forces at matrix cracks. Delamination growth is mainly driven by interlaminar shear stresses (mode II) induced by the bending of the laminate during the impact event. Finally, fibre fracture can be a significant energy absorbing mechanism, particularly at high velocities, and is generated by the high through-thickness forces generated during impact. Fibres can either fail in tension due to the membrane forces generated during impact, or by shear-out during penetration of the impactor [4].

One of the factors thought to contribute to the susceptibility of composites to delamination is the brittle nature of the matrix resins generally employed. Enhancing the fracture resistance of CFRPs has received considerable attention in recent years. For example, by employing rubber interleaves on unidirectional carbon prepreg systems Seferis [5] found the damage area resulting from impact to be reduced., Walker et al [6] used different types of short fibers (PA web/Kevlar/zylon/PEEA) and randomly and evenly distributed them in the interlaminar region. They succeed in reducing the visible damage and the detectable damage. Sohn and Hu [7] used chopped kevlar fibres of 5-7

mm in length and 18gmp<sup>2</sup> in weight-to-area ratio as the third-dimension reinforcing fibres in a CFRP. The presence of the chopped kevlar fibres reduced the compressive strength but increased the delamination toughness by over 100%. Moreover Sohn and Hu [8] have showed that spreading small amounts of chopped Kevlar fibres between continuous-carbonfibre layers can improve the mode II delamination toughness, which is achieved by the more pronounced crack growth resistance R-curve behaviour. Another method of increasing the impact resistance of composites is the Z-pinning. On the one hand, Z-pinning not only improves the delamination toughness, but has the added benefit of transforming the crack propagation from an unstable (i.e., fast fracture) to stable process in brittle matrix laminates, which is a desirable property in damage tolerant structures. On the other hand, Z-pinning is not effective at resisting the initiation and growth of short delamination cracks, but is remarkably effective at resisting the propagation of long delamination cracks (typically larger than 2–5 mm)[9]. Stitching has also been proved to greatly reduce the damage area and to slightly improve the compression after impact (CAI) [10].

Recently the researchers have turned their attention to nanofillers because of their exceptional properties i.e. carbon nanofibres, nanoclays and carbon nanotubes, in order to enhance the fracture properties of polymers and composites. Especially since the discovery of Carbon Nanotubes (CNTs), they have attracted the attention of the researchers worldwide because of their superb properties. Their large aspect ratio, surface area and high Young Modulus are believed to be the key candidates for improving the fracture behaviour of CFRPs when they are used as fillers for polymeric matrices. Iwahori et al. [11] introduced cup stacked nanofibres (CSNF) in 10% w.t. in a CFRP and demonstrated improved compression and flexural properties. Kostopoulos et al.[12] verified an increase of 100% in fracture energy was observed after the addition of 1% CNF in the matrix of the laminates. The investigation of the fracture surfaces showed extensive fiber bridging because of the presence of CNFs, which verified the enhanced fracture properties. Similar research by Sadeghian et al. [13] proved the positive effect on the fracture properties of glass/polyester composite manufactured by VART with the addition of 1% w.t. CNF. Siddiqui et al [14] used organoclay modified epoxy that in turn gave rise to significant improvements in both crack growth resistance and fracture toughness of mode I interlaminar fracture of CFRP composites. Arai et al [15] with the use of carbon nanofibre interlayer in CFRP laminates improved the fracture toughness under mode I and mode II loading significantly. Gojny et al [16-17] incorporated SWCNT, DWCNT and MWCNT in an epoxy resin in 0.1 to 1 % w.t and dramatically enhanced the fracture toughness of the resin. While Wichman et al. [18] even though found that the addition of MWCNTs in 0.3% w.t. in glass/polyester composite via RTM improved the shear properties, no actual improvement was recorded for mode I and mode II fracture tests. Yokozeiki et al. [19] on the other hand used CSNT in large weight fractions (5 and 10% w.t) in UD carbon prepreps and performed fracture and impact test. The results revealed slightly reduced delamination areas and improved fractured properties for the nanodoped composite.

It is clear that the investigation of the impact properties of CFRPs with CNTs incorporated into the polymer matrix has not been thoroughly investigated so far. The current study investigated the influence of Multi-Wall Carbon Nanotubes (MWNTs) on the impact behaviour of quasi-isotropic CFRPs. The nanotubes were incorporated in the epoxy matrix of the laminates in 0.5% per weight concentration via a high shear mixing device and drop tower impact tests were performed for various energy levels ranging from 8 to 20 Joules.

## 2. EXPERIMENTAL

### 2.1. Materials

MWCNTs produced by catalysed CVD, were supplied by ARKEMA, France. Their diameters were 10-15 nm and they were more than 500 nm long, resulting in a dimensional ratio length to diameter of 30-50. The nanotubes were dried in an oven overnight prior to use. The epoxy system used for the fabrication of CNT doped resins was the Araldite LY564/ Aradur HY2954 from Huntsman Advanced Materials, Switzerland.

### 2.2. Specimen preparation

The dispersion of the MWCNTs in the epoxy took place in a Torus Mill device (VMA Getzmann GmbH). The torus mill introduces high shear forces by a high-speed rotating disc and reduces the nanoparticle agglomerates due to the milling effect generated by zirconium dioxide beads. The beads have a diameter of 1.2 to 1.7 mm and cause strong shear action and collision effects. The dissolver-disc provides additional shear forces and maintains the vortex flow. The compound is stirred in a vacuum container to avoid air inclusion. The vortex flow achieved by the geometry of the disc leads to continuous mixing of the compound. The mixing speed was at 2000 rpm for 3 h and the CNT content was 0.5 %.

The manufacturing of CFRPs with the above resin as matrix material was the next step. The Carbon Fibre (CF) laminas were chosen to be quasi-isotropic  $[0/+45/-45/90]_2$ , of 16 plies by Wela, Germany with weight of 160 gr/m<sup>2</sup>. Each panel was hand laid-up and then processed in an autoclave, using the vacuum bag technique. A reference panel was also manufactured with neat resin for direct comparison. In total there were two batches of specimens tested; one having a modified matrix with the addition of CNT and the other having an unmodified matrix. The CFRPs had a thickness of 2mm and the test specimens cut were at 80x80 mm<sup>2</sup>. The waterjet method was used to cut the specimen from the prepared plates.

### 2.3. Impact testing, evaluation and CAI

The impact tests were performed at a drop tower using a hemispherical impactor, weighing 3.01kg (constantly), according to ASTM D5628-07. The tests were automated and the machine employed for these tests was a Fractovis – Instrumented falling weight tester at IVW provided by CEAST.

In order to select the five (5) energy levels to be tested, the impact damage threshold had to be determined. Using the Barely Visible Impact Damage (BVID) approach, the impact damage threshold was estimated to be at 4 Joules approximately. This was a result of consecutive impacts, starting from 1 Joule with unit intervals and examining for any visible damage after every impact. Thereafter, the impact energy levels were defined resulting in a number of distinct levels; one below BVID threshold and 4 above it; 2, 8, 12, 16 and 20 Joules. To achieve the required impact energy the initial height of the impactor was variable and was adjusted accordingly. During the tests, the acceleration, force, velocity, deformation and energy versus time were recorded and calculated automatically.

After the impact testing, the next step involved the examination of the impacted specimens using non destructive techniques; mainly C-Scan (model) and an Optical System Measuring System. The Optical System Measuring System used was MicroProf® Profilometer provided by FRT GmbH. By scanning the surface of a specimen, the equipment makes non-contact measurements by using laser and white light sensors. Measurements include roughness, elevation profile, contours, bumps etc. For the present study we measured the imp actor's print on the specimen surface, its

diameter and depth, together with the back face bumps created. With the use of accompanying software i.e. FRT Mark III the C-Scan images were post-processed and data regarding delamination areas and mean diameter of damage were extracted. These, in combination with the recorded data during the impact, were utilized to characterize the overall performance of the materials under impact.

After the impact induced damage was measured and evaluated, the specimens were subject to Compression After Impact (CAI) tests. In search for further data, some specimens were subject to Compression Fatigue After Impact (FCAI). These tests were performed according to the ASTM D7137M-07.

### 3. RESULTS & DISCUSSION

In order to detect any changes in the performance of the different materials under impact loading, various parameters were used. The parameters of this investigation included the peak response force, the resulting delamination area (as measured through C-Scan), the absorbed energy and its percentage. Finally, as the energy required for the creation of a delamination under impact loading is related to the fracture toughness of the composite, the specific energies for delamination, (the energy required to create the delamination), were compared.

#### 3.1. Peak Impact Force

Fig.1 presents the measured the peak impact values experienced by the specimens during impact. Peak forces do not show differences between two groups of materials. The time responses of the two groups due to dynamic impact load do not show differences such as delays or changes in the general pattern of the curve. Furthermore, the force values at 12, 16 and 20 Joules seem to be gathered around 6kN without showing extensive changes. Bearing in mind that the change in energy is due to impact velocity change, it can be stated that there is a threshold energy after which the impact response force does not increase further, as it can be seen from 2 to 8 Joules.

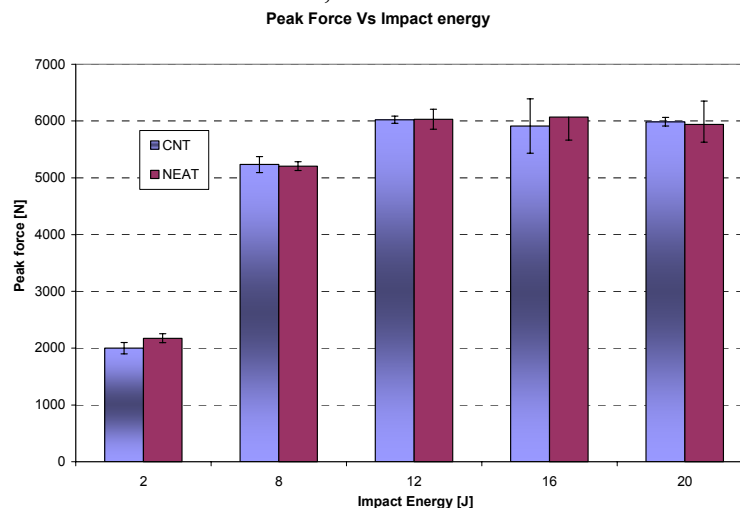
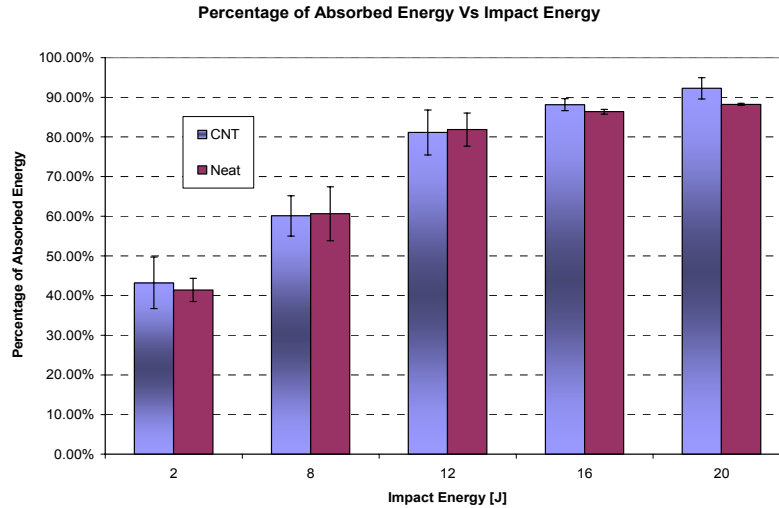


Figure 1: Peak Force versus Impact energy levels for both the CNT doped specimens and the neat ones.

#### 3.2. Absorbed Energy

From the response of the material, we compute the absorbed energy. This information is can be extracted from a force – displacement diagram by calculating the area between the loading and unloading curve. The results of these calculations normalized to the impact energy are presented in Fig.2. In the figure of the Percentage of Absorbed energy, the presence of CNT in the matrix of the composite is becoming more obvious.

More precisely, at the lower impact energies (2, 8, 12 J), it can be seen that no major differences can be noted. However, while the incident energy increases further, to 16 and 20 J, the modified composites show a better absorption performance. There is a tendency for the two groups of materials to differ. The energy absorbed by the CNT doped composites represents a larger amount of the impact energy. This percentage reaches 92.5% at 20J.



**Figure 2: Percentage of Absorbed Energy versus Impact energy levels for both the CNT doped specimens and the neat ones.**

### 3.3. C-scan and Impact Delamination Area

As mentioned above, C-scan measurements followed the impact tests in order to evaluate the impact induced damage. Through these measurements, we got information on the areas affected by the impact. However no information on the thickness direction can be extracted as the maps created are projections of the various delaminations present between the different laminates of the composite.

The following pictures present the comparison of the delamination energies between the two groups of specimen at the different impact energies. The shaded background pictures are the non-modified matrix composites, while the foreground shows the outline of the delamination created in the modified matrix composites.

On almost all the C-scan maps, a small defective area on the top edge of the specimens can be seen. This was a delamination created during the machining of the specimens due to the waterjet beam. A general note is that the areas of the composites with the CNT doped matrix tend to be smaller than the un-doped composite. Nano-enhancement in the matrix, which is closely related to CNT breakage and CNT pulling-out, seems to prevent development of extensive delamination. At higher energies, presence of CNT shows that propagation of delamination stops earlier resulting in a reduced delamination area, while the impact forces remain at the same level as already mentioned.

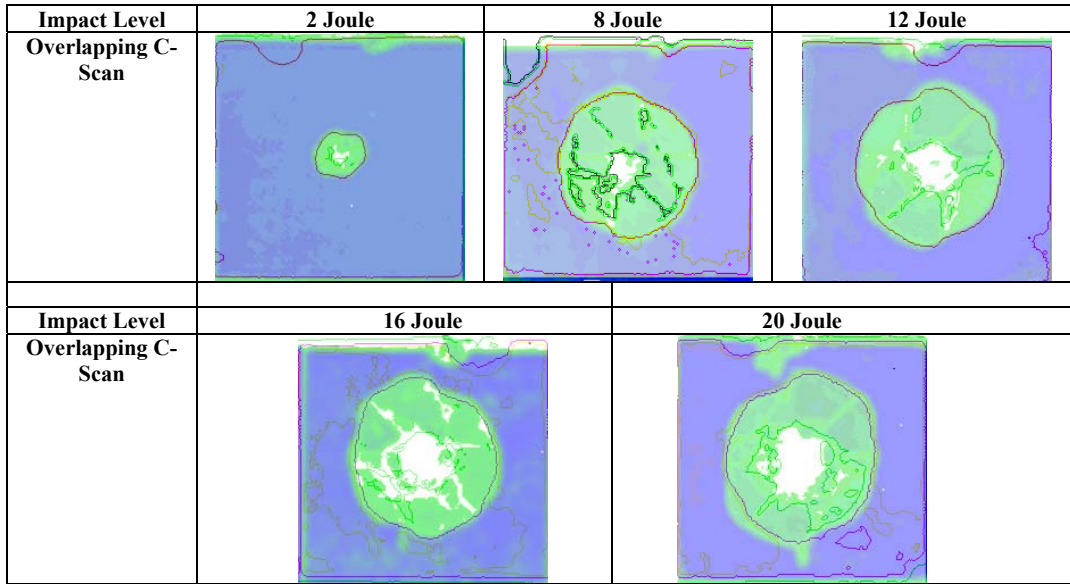


**Figure 3: C-Scans of impacted specimens at all energy levels for comparison of the delamination areas for the cnt-doped and undoped specimens.**

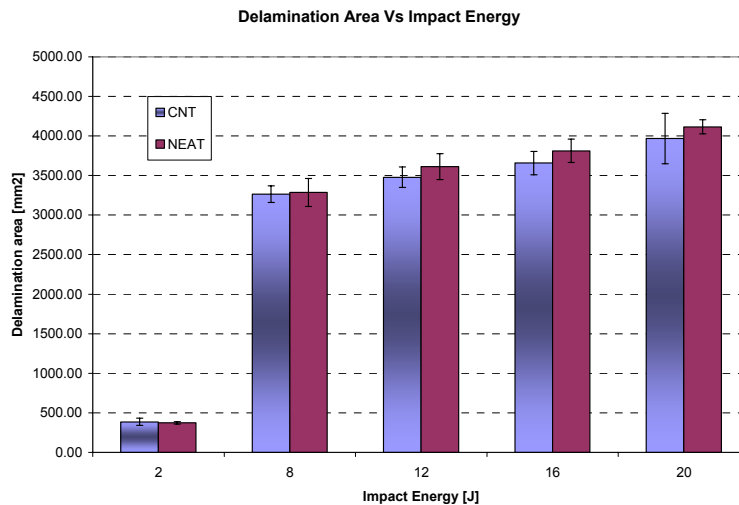


**Figure 4: Delamination Area versus Impact energy levels for both the CNT doped specimens and the neat ones.**

The areas were accurately measured using post-processing software able to track contours of the given maps. The gathered results are shown in Fig.4. Based on the measurements of Fig.4, on almost all impact levels the delamination area of the nano-doped matrix is smaller than the un-doped. Moreover, the differences between the two groups seem to become larger as the impact energy increases. This observation can be attributed to the large interface area that CNT provide. The large surface area of the CNTs absorbs more energy than the neat specimens, while their large aspect ratio contributed to the minimisation of the delamination area by arresting, blunting the developing cracks. This can be justified by the Scanning Electron Microscopy pictures, presented below, that show the presence of CNT on the fractured interface and the CNTs extruding from the resin, at the bottom SEM picture of higher magnification.

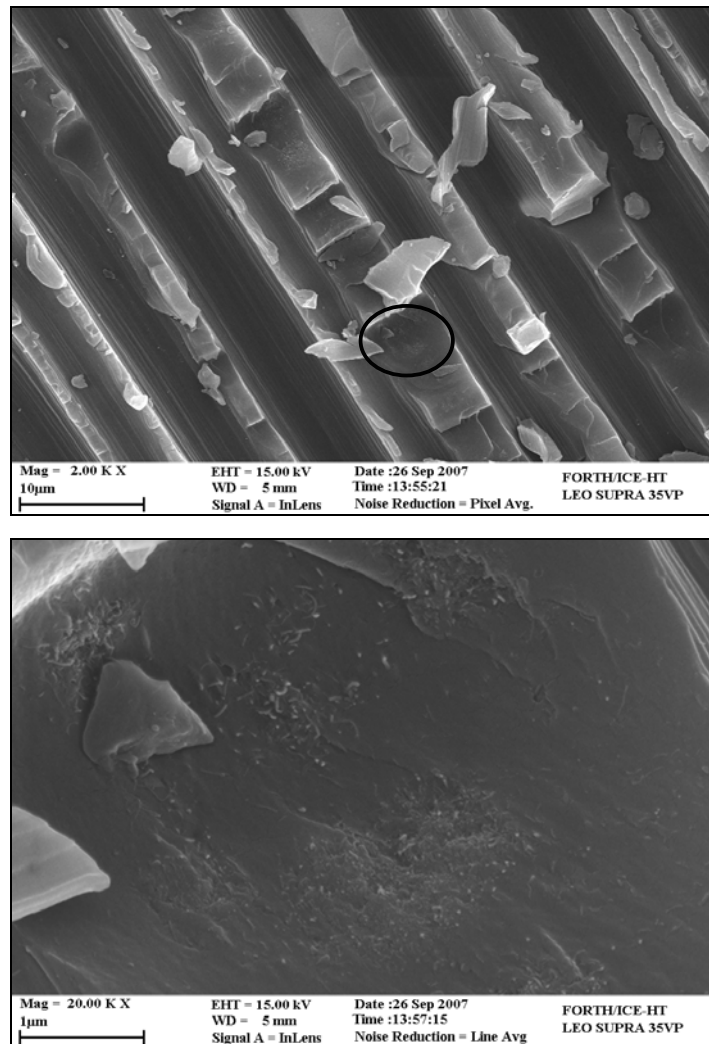


**Figure 5: Indicative SEM micrographs of impacted specimen with 0.5% w.t. MWCNT at 16Joule at two magnifications. At the bottom picture (zoomed in area of the black circle of the upper picture) the fractured and pulled-out CNTs that contribute to higher impact and CAI properties, are obvious.**

### **3.4. Specific Delamination Energy**

Evaluating further the results and data collected, we defined Specific Delamination Energy as the energy required to develop a delamination of area unit (as measured by C-scan); in our case resulting in a value of  $J/m^2$ . Through this, it was attempted to relate the energy to the area, just as in the fracture tests.

Although this attempt did not give valuable information at low energies, at 20J impact energy the specific delamination energy of the CNT doped composite clearly distinguished. Meaning that the energy required developing a certain amount of delamination increased rapidly for the CNT doped composite, while for the un-doped the specific delamination energy followed a more linear trend.

Another interesting point is the fact that both groups of materials show a decrease in the specific delamination energy from the 2J impact to the 8J impact. This can be explained by the fact that the area used in the calculations is the one measured by C-scan which is the projected area of the delaminations. The delamination not only expands parallel to the specimen's reference plain but also delaminations are created along the through thickness direction.

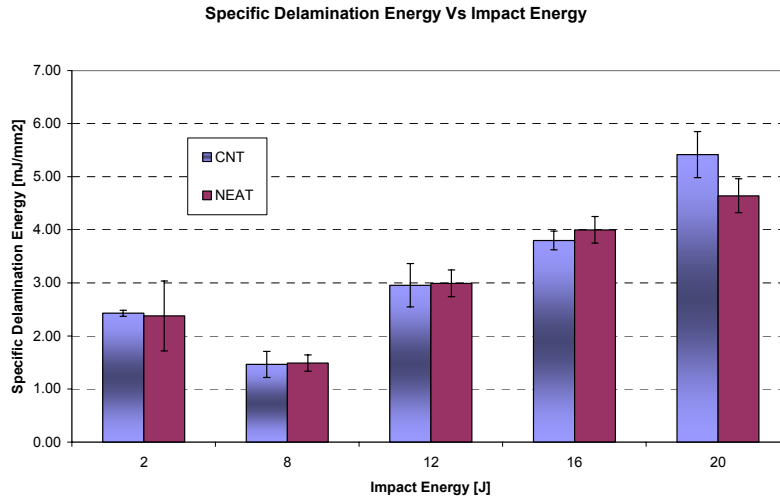


**Figure 6: Specific Delamination Energy versus Impact energy levels for both the CNT doped specimens and the neat ones.**

### 3.5. Compression After Impact (CAI)

From these tests, we estimated the effective modulus of the impacted specimens. It is clear that the CNT-doped specimens have improved properties when directly compared with the neat resin ones. In more detail the inclusion of the CNTs has increased the CAI modulus about 13-17%. Once again the mechanical properties of the CNTs and the failure mechanisms i.e breakage, telescopic fracture and pull-out are the main reason for the aforementioned enhancement.

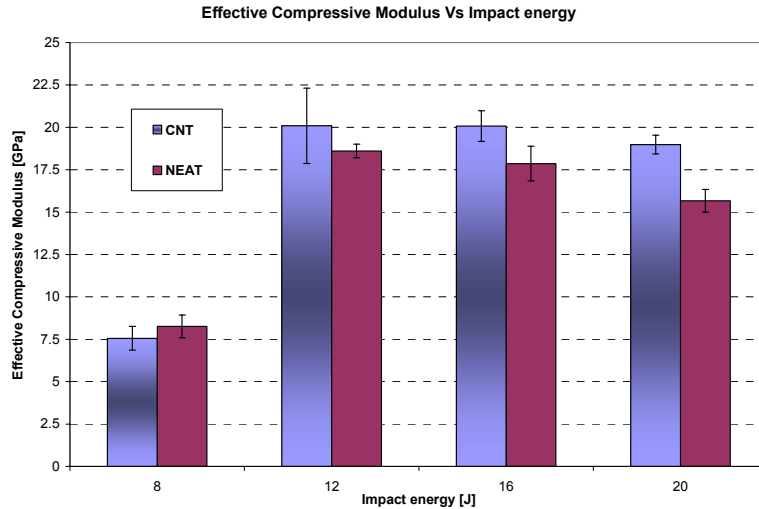


**Figure 7: Effective Compressive Modulus versus Impact energy levels for both the CNT doped specimens and the neat ones.**

## 4. CONCLUSIONS

Quasi-isotropic CFRP laminates doped with 0.5% w.t. MWCNTs were manufactured using typical hand lay-up and autoclave techniques. The produced specimens were subjected to low velocity impact using a drop tower and finally tested under compression after impact (CAI). It has already been proven in the literature that the inclusion of CNTs into a polymer matrix enhances the fracture toughness under Mode I and Mode II. Mode I and II dominate the impact failure mechanisms and therefore it

was strongly believed that the positive effect of the CNTs was feasible to be directly transferred onto the impact properties of a CFRP.

However at low velocity impact no significant difference was observed for the delamination area or the absorbed area when directly comparing the neat and the doped specimens for low energy impact levels. The reinforcing effect of the CNTs seems to be more pronounced for higher impact energy levels. Therefore impact tests should be performed with higher energy levels or high velocity impact to investigate further the effect of the CNTs. On the other hand the effective compressive modulus after impact was improved about 13-17% for all the CNT doped specimens compared with the neat resin. The extensive fibre pull-out and fibre breakage of the CNTs during compression loading are the main reasons for the aforementioned improvement.

## 5. ACKNOWLEDGEMENTS

The financial support of the FP6 EU-STREP project NOESIS is acknowledged. This research project is co-financed by E.U.-European Social Fund (75%) and the Greek Ministry of Development-GSRT (25%). Special thanks go to Mr. F.Kempel of IWV, Kaiserslautern, Germany for his immense help with the impact drop tower tests.

## REFERENCES

1. M. O. W. Richardson and M. J. Wisheart (1996) Review of low-velocity impact properties of composite materials. *Composites Part A* 27A 1123-1131
2. Derek Hull & Yi Bing Shi (1993) Damage mechanism characterization in composite damage tolerance investigations. *Composite Structures* 23 (1993) 99-120
3. Greenhalgh E. (1998) Characterisation of mixed-mode delamination growth in carbon fibre composites. PhD Thesis Imperial College.
4. Greenhalgh E., Hiley M. (2003) The assessment of novel materials and processes for the impact tolerant design of stiffened composite aerospace structures. *Composites: Part A* 34 151-161
5. Eric N. Gilbert, Brian S. Hayes, James C. Seferis (2003) Interlayer toughened unidirectional carbon prepreg systems: effect of preformed particle morphology. *Composites: Part A* 34 245-252
6. L. Walker, M.-S. Sohn, X.-Z. Hu (2002) Improving impact resistance of carbon-fibre composites through interlaminar reinforcement. *Composites: Part A* 33 893-902
7. Min-Seok Sohn & Xiao-Zhi Hu (1998) Processing of carbon-fibre/epoxy composites with cost-effective interlaminar reinforcement. *Composites Science and Technology* 58 211-220
8. Min-Seok Sohn & Xiao-Zhi Hu (1994) Mode II delamination toughness of carbon/epoxy composites with chopped Kevlar fiber reinforcement. *Composites Science and Technology* 52 439-448
9. A.P. Mouritz (2007) Review of z-pinned composite laminates. *Composites: Part A* 38 2383-2397
10. Joon-Hyung Byun, Sung-Wook Song, Chang-Hoon Lee, Moon-Kwang Um, Byung-Sun Hwang (2006) Impact properties of laminated composites with stitching fibers. *Composite Structures* 76 21-27
11. Yutaka Iwahori, Shin Ishiwata, Tomoji Sumizawa, Takashi Ishikawa (2005) Mechanical properties improvements in two-phase and three-phase composites using carbon nano-fiber dispersed resin. *Composites: Part A* 36 1430-1439

12. S. Tsantzalīs, P. Karapappas, A. Vavouliotis, P. Tsotra, V. Kostopoulos, T. Tanimoto, K. Friedrich (2007) On the improvement of toughness of CFRPs with resin doped with CNF and PZT particles. *Composites: Part A* 38 1159–1162
13. Sadeghian R, Gangireddy S, Minaie B, Hsiao KT (2005) Manufacturing carbon nanofibers toughened polyester/glass fiber composites using vacuum assisted resin transfer molding for enhancing the mode-I delamination resistance. *Composites Part A*:
14. Naveed A. Siddiqui, Ricky S.C. Woo, Jang-Kyo Kim, Christopher C.K. Leung, Arshad Munir (2007) Mode I interlaminar fracture behavior and mechanical properties of CFRPs with nanoclay-filled epoxy matrix. *Composites: Part A* 38 449–460
15. Masahiro Arai, Yukihiro Noro, Koh-ichi Sugimoto, Morinobu Endo, (2008) Mode I and mode II interlaminar fracture toughness of CFRP laminates toughened by carbon nanofiber interlayer. *Composites Science and Technology* 68 516–525
16. Gojny FH, Wichmann MHG, Fiedler B, Schulte K, (2005) Influence of different carbon nanotubes on the mechanical properties of epoxy matrix composites-A comparative study. *Composites Science and Technology*: 65: 2300-2313.
17. Gojny FH, Wichmann MHG, Kopke U, Fiedler B, Schulte K, (2004) Carbon nanotube –reinforced epoxy composites: enhanced stiffness and fracture toughness at low nanotube content. *Composites Science and Technology*: 64: 2363-2371.
18. Wichman MHG, Sumfleth J, Gojny FH, Quaresimin M, Fiedler B, Schulte K, (2006) Glass-fibre reinforced composites with enhanced mechanical and electrical properties- Benefits and limitations of a nanoparticle modified matrix. *Engineering Fracture Mechanics*: 73: 2346-2359.
19. Tomohiro Yokozeki, Yutaka Iwahori, Shin Ishiwata, Kiyoshi Enomoto (2007) Mechanical properties of CFRP laminates manufactured from unidirectional prepreps using CSCNT-dispersed epoxy. *Composites: Part A* 38 2121–2130